JJMIE

Volume 9 Number 1, February.2015
ISSN 1995-6665
Pages 61- 66

Jordan Journal of Mechanical and Industrial Engineering

Combustion Modeling with CFD in Direct Injection CI Engine Fuelled with Biodiesel

Ajay V. Kolhe *, Rajesh E. Shelke , S. S. Khandare

Dept. of Mechanical Engineering, Kavikulguru Institute of Technology and Science, Ramtek, Dist. Nagpur, India, Govt. ITI Vocational training institute, Daryapur, Dist. Amravati, B. D. College of Engineering Sewagram.

Received 19 Feb 2014 *Accepted 31 Jan 2015*

Abstract

The present paper describes the development of sub models for combustion analysis in direct injection (DI) diesel engine fuelled with Pongamia Pinnata biodiesel-diesel blend as a fuel. In the present study, the Computational Fluid Dynamics (CFD) code FLUENT was used to model a complex combustion phenomenon in Compression Ignition (CI) engine. The experiments were performed on a single cylinder direct injection diesel engine, with a full load condition at a constant speed of 1500 rpm. Combustion parameters, such as cylinder pressure and heat release rate, were obtained from experimental data. The numerical modeling was solved by CFD code Fluent, taking into account the effect of turbulence. For modeling turbulence Renormalization Group Theory (RNG) k-ε model was used. The sub models such as droplet collision model and Taylor Analogy Breakup (TAB) model were used for spray modeling. Modeling in cylinder combustion, species transport and finite rate chemistry model were used. The results obtained from modeling were compared with experimental investigation. The peak modeling heat release rate was 30 J/s whereas the experimental peak heat release rate was 25 J/s at 364 degree CA for biodiesel. Similarly, for the diesel peak modelling, the heat release rate was 34.41 J/s whereas the experimental peak heat release rate was 27 J/s at 364 degree CA. Simulated results including the in-cylinder pressure, rate of pressure rise and heat release rate profiles have been analysed. A good agreement between the modelling and experimental data ensures the accuracy of the numerical predictions collected in this work. Including peak values of in-cylinder pressure, rate of pressure rise and heat release rate shows a good agreement between modelling and the measured data. All in all, this study demonstrates the feasibility of integrating a compact multi-component surrogate fuel mechanism with CFD to elucidate the in-cylinder combustion of biodiesel fuels.

Keywords: *Biodiesel, CFD, DI, Heat Release Rate, Peak Pressure*.

Abbreviations

θ	Crank angle, degree
μ	Dynamic viscosity
v	Kinematic viscosity
ρ	Density
ϕ	Equivalence ratio
Q_n	Net heat release
Q_w	Heat transfer to the cylinder wall
Q_g	Gross heat release
RNG	Renormalization Group Theory

1. Introduction

The combustion research is more extensive, diverse and interdisciplinary due to a powerful modeling tool like the Computational Fluid Dynamics (CFD). In CI engine, the in-cylinder multiphase fluid dynamics like fuel spray, chemical reaction kinetics influence the combustion. The fluid flow in an internal combustion engine presents one of the most challenging fluid dynamics problems to the model. This is because the flow is associated with large density variations. So, a detailed understanding of the flow and combustion processes is required to improve the performance of the engine [7,9]. Substantial differences in viscosity, surface tension, density and thermal conductivity were obtained relative to reference diesel fuels and among the different source materials. The combustion model revealed differences in the temperature and emissions of biodiesel when compared to reference diesel fuel [1-8]. The combustion chamber flow field and its effect on fuel spray characteristics play an important role in improving the efficiency and reducing the pollutant emission in a direct injection diesel engine, in terms of influencing processes of breakup, evaporation, mixture formation, ignition, combustion and pollutant formation. CFD modeling was a valuable tool for acquiring detailed

* Corresponding author. e-mail: ajay.kolhe4@gmail.com.

information about these important processes [2,5]. The longer ignition delay leads to a rapid burning rate and the pressure and temperature inside the cylinder rise suddenly. Hence, most of the fuel burns in premixed mode causes a maximum peak heat release rate, a maximum cumulative heat release and a shorter combustion duration [9-17]. The CFD results clearly indicate the impact of the system parameter variations on the NO and soot emission characteristics and the ability of the adopted models to reflect the results sensitivity [18]. The simulation carried out in the present work to model DI diesel engine with bowl in piston for a better understanding of the in-cylinder gas motion with details of the combustion process. An attempt was made to study the combustion processes in a compression ignition engine; a simulation was done using CFD code FLUENT, Turbulent flow modeling and combustion modeling were analyzed in formulating and developing a model for the combustion process by using Karanja biodiesel and diesel blend.

2. Experimental Set Up

The schematic diagram of the experimental set up was shown in Figure 1. The engine was of a single cylinder four stroke direct injection water cooled diesel engine. The engine has rated output 5.2 kW at speed 1500 rpm with compression ratio 17.5, injection pressure 180 kg/cm^2 and coupled with rope brake dynamometer. The detailed specification of the engine is given in Table 1. Performance tests were carried out on compression ignition engine using various blends of biodiesel and diesel as a fuel.

3. Geometry Development and Meshing of Computational Domain

In the present study, geometry is modeled in preprocessor by using a workbench tool design modeler and then meshed in ICEM, respectively. Figure 2 shows the computational domain of two dimensional combustion chamber geometry counting inlet and exhaust ports. Both intake ports have been meshed with the same orientation in the flow direction and they were joined with a cylindrical structured mesh in the zone upstream of the valves. The combustion chamber is bowl in piston type, which has a hemispherical groove on piston top.

The geometry was modeled at its zero crank angle position at TDC as shown in Figures 2 and 3. In ICE, it was necessary that, for obtaining realistic simulations, the computation must include a combustion chamber geometry with an inlet and an exhaust valve. The computations performed on bowl in piston type combustion chamber reveled that, instead of suction stroke at the end of compression stroke, the geometry plays an important role to access the combustion when both the valves were closed.

4. Model Development

In the present paper, the problem is attempted to be solved as an unsteady first order implicit with turbulence effects considered to simulate the combustion for CI, DI engine. The numerical methodology was a segregated pressure based solution algorithm. For solving species, the discrete phase injection with species transport equation and finite rate chemistry reactions were used. The upwind scheme was employed for the discretization of the model equations. FLUENT uses a control volume based technique to convert the governing equations to algebraic equations that can solve numerically. The governing equations for mass, momentum and energy equations were used and appropriate initial boundary conditions were chosen for the combustion analysis [15,19].

4.1. Turbulance Model

Turbulence was distinguished by the fluctuation of the velocity field. In the present work, the well-known RNG *k-ε* model was used for modelling turbulence. The RNG *k-ε* model was derived using a thorough statistical technique. It was analogous in form to the standard *k-ε* model but had the advantage of including effect of swirl, which was important for ICE combustion analysis. Transport equations for the RNG *k-ε* Model were defined as:

$$\frac{\partial}{\partial t}(\rho k)+\frac{\partial}{\partial x_i}(\rho k u_i)=\frac{\partial}{\partial x_i}\left[(\mu+\frac{\mu_t}{\sigma_k})\frac{\partial k}{\partial x_j}\right]+P_k-\rho\epsilon \quad (1)$$

$$\frac{\partial}{\partial t}(\rho\epsilon)+\frac{\partial}{\partial x_i}(\rho\epsilon u_i)=\frac{\partial}{\partial x_j}\left[\left(\mu+\frac{\mu_t}{\sigma_\epsilon}\right)\frac{\partial\epsilon}{\partial x_j}\right]+C_{1\epsilon}\frac{\epsilon}{k}P_k-C_{2\epsilon}^{*}\rho\frac{\epsilon^2}{k} \quad (2)$$

Where, $C_{2\epsilon}^{*}=C_{2\epsilon}+\frac{C_\mu \eta^3(1-\eta/\eta_0)}{1+\beta\eta^3}$

4.2. Combustion Modeling

The ignition/combustion model was based on a modified Eddy Dissipation Concept (EDC) which was implemented into the CFD code. Multiple simultaneous chemical reactions can be modelled, with reactions occurring in the bulk phase (volumetric reactions) and/or on wall surfaces [13,16]. The conservation equation takes the following general form:

$$\frac{\partial}{\partial t}(\rho Y_i)+\nabla.(\rho\vec{v}Y_i)=-\nabla.\vec{J}_i+R_i-S_i$$

where *Ri* is the net rate of production of species *i* by chemical reaction and S_i is the rate of creation by addition from the dispersed phase.

4.3. Engine Ignition Modeling

For the present study the auto-ignition model (Harden-burg model) was the most suitable for simulating a direct injection diesel engine. The transport equation for an ignition species Y_{ia} is given by:

$$\frac{\partial}{\partial t}(\rho Y_{ig})+\nabla.(\rho\vec{v}Y_{ig})=-\nabla.\frac{\mu_t}{S_{ct}}(\nabla Y_{ig})+(\rho S_{ig})$$

where Y_{ig} is a "mass fraction" of a passive species representing radicals which form when the fuel in the domain breaks down. S_{ct} is the turbulent Schmidt number. The term S_{ig} is the source term for the ignition species which has the form:

$$S_{ig}=\int_{t=t_0}^{t}\frac{dt}{\tau_{ig}}$$

4.4. Spray Break Up Model

In the present work, TAB model was used. The TAB model was based on the analogy between an oscillating and distorting droplet and a spring mass system. The distorting droplet effect was considered in the present study. The equation governing a damped, force oscillator is:

$$F - kx - d\frac{dx}{dt} = m\frac{d^2x}{dt^2}$$

where the displacement of the droplet equator from its spherical position and the coefficients of this equation are taken from Taylor's analogy:

$$\frac{F}{m} = C_F\frac{\rho_g\mu^2}{\rho_l r}, \frac{k}{m} = C_k\frac{\rho}{\rho_l r^3}, \frac{d}{m} = C_d\frac{\mu_l}{\rho_l r^2}$$

where ρi and ρa are the discrete phase and continuous phase densities, V_r was the relative velocity of the droplet, r was the undisturbed droplet radius, σ was the droplet surface tension and μ_i was the droplet viscosity [16,17].

4.5. Droplet Collision Model

The droplet collision model includes tracking of droplets for estimating the number of droplet collisions and their outcomes in a computationally efficient manner. The model is based on O'Rourke's method, which assumes stochastic approximation of collisions [14-17]. When two parcels of droplets collide an algorithm further establishes the type of collision. Only coalescence and bouncing outcomes are measured. The probability of each outcome was calculated from the collision Weber number and fit to experimental observations. The Weber number was given as:

$$W_e = \frac{\rho V_r^2 l}{\sigma}$$

where V_r is the relative velocity between two parcels and l is the arithmetic mean diameter of the two parcels. The state of the two colliding parcels is modified based on the outcome of the collision.

4.6. Wall Film Model

The spray wall interaction is an important element of the mixture creation process in diesel engines. In a DI engine, the fuel was injected directly into the combustion chamber, where the spray can impinge upon the piston. The modeling of the wall film inside a DI engine was compounded by the occurrence of carbon deposits on the surfaces of the combustion chamber. This carbon deposit soak up the liquid layer. It was understood that the carbon deposits adsorb the fuel later in the cycle. The wall film model in FLUENT allows a single constituent liquid drop to impinge upon a boundary surface and form a thin film. Interactions during impact with a boundary and the criteria by which the regimes are detached are based on the impact energy and the boiling temperature of the liquid [13-17]. The impact energy is defined by:

$$E^2 = \frac{\rho V_r^2 D}{\sigma}\left(\frac{1}{\min(h_0/D, 1) + \delta_{bl}/D}\right)$$

where ρ is the liquid density, V_r is the relative velocity of the particle in the frame of the wall, D is the diameter of the droplet, and s is the surface tension of the liquid. Here, dbl is a boundary layer thickness.

5. Engine Specifications

Table 1. Engine Specifications

Specification	Details
Number of strokes	4
Power output	5.2 kW / 7BHP
Bore x Stroke	87.5 mm x 110 mm
Number of cylinder	One
Dynamometer	Mechanical loading
Drum diameter	35 cm
Orifice diameter	20 cm
Coefficient of discharge	0.6
Injection pressure	180 – 200 bar

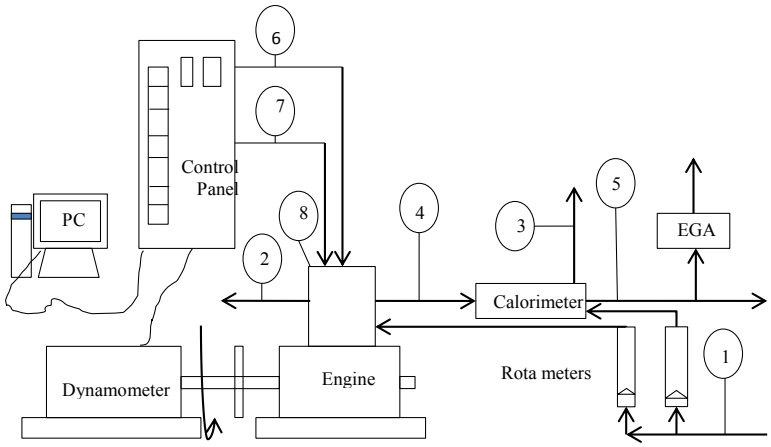

Figure 1. Schematic diagram of experimental set up.

1) Water inlet to the calorimeter and engine (T_1°C)
2) Water outlet from the engine jacket (T_2°C)
3) Water outlet from the calorimeter (T_3°C)
4) Exhaust gas inlet to the calorimeter (T_4°C)
5) Exhaust gas outlet from the calorimeter (T_5°C)
6) Atmospheric air temperature (T_6°C)
7) Fuel flow
8) Pressure transducer, EGA- Exhaust gas analyser

6. Properties of Liquid Fuel Droplet

Table 2. Properties of liquid fuel droplet

Droplet properties	Diesel	PME
Density (kg/m^3)	850	876
Specific heat capacity (J/kg.K)	2090	1810
Thermal conductivity (W/m.K)	0.149	0.158
Viscosity (kg/m.s)	0.004	0.006
Latent heat (J/kg)	277,000	231,436
Vaporisation temperature (K)	341	341
Boiling point (K)	447.10	664.65
Volatile component fraction (%)	100	100
Binary diffusivity (m^2/s)	3.79 ×10^{-6}	7.42×10^{-6}
Saturation vapour pressure (Pascal)	1329	1329
Droplet surface tension (N/m)	0.02521	0.02616
Critical temperature (K)	617.7	832.3
Critical pressure (Pascal)	2,110,000	1,307,500
Critical specific volume (m^3/kg)	0.004386	0.003740

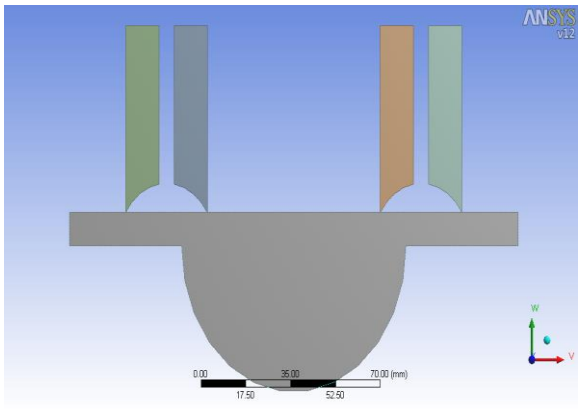

Figure 2. Geometry of combustion chamber with valves

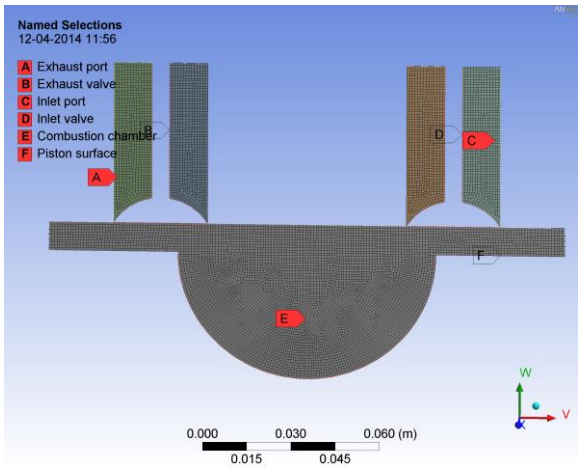

Figure 3. Mesh structure of computational domain for model geometry

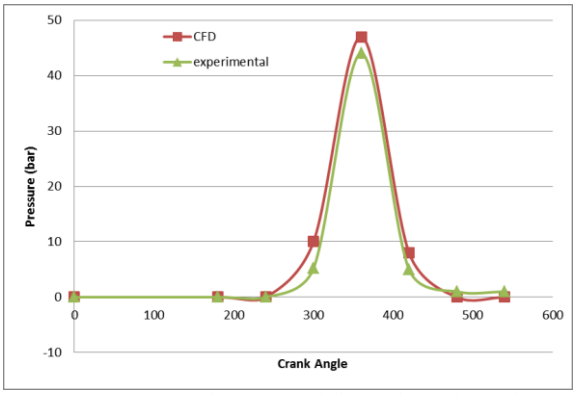

Figure 4. Comparisons between modeling and experimental pressure (*p-θ*) diagram of Biodiesel blend

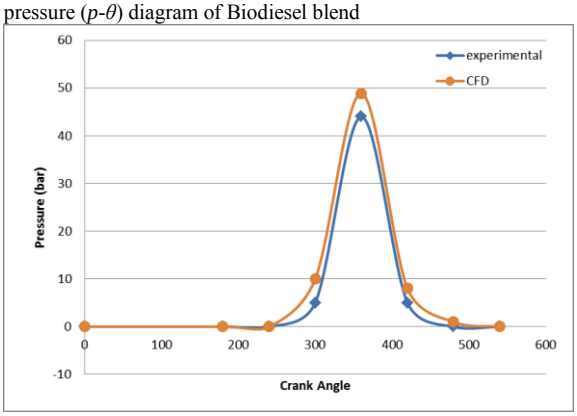

Figure 5. Comparisons between modeling and experimental pressure (*p-θ)* diagram of Diesel

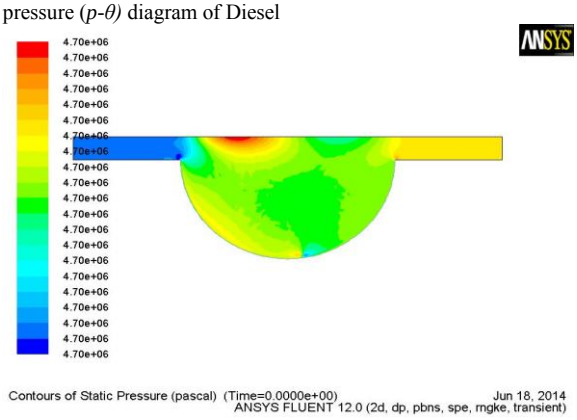

Figure 6. Pressure distribution in (Bar) CA = 360^0 (max. Load) for biodiesel blend

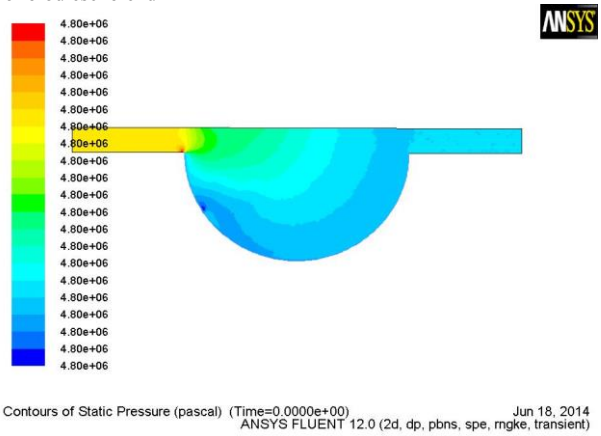

Figure 7. Pressure distribution in (Bar) CA = 360^0 (maximum load) for Diesel

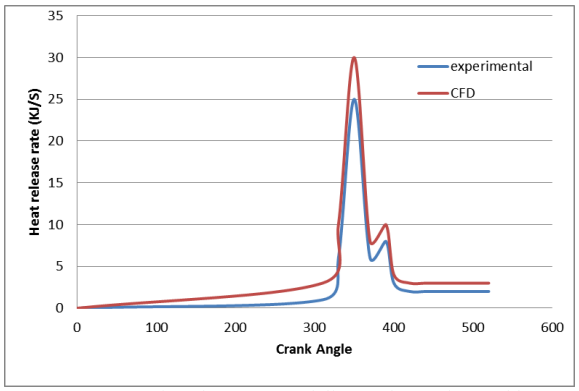

Figure 8. Comparison between modeling and experimental heat release rate for biodiesel blend

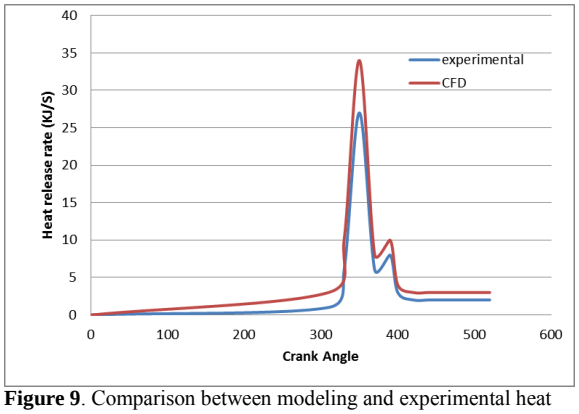

Figure 9. Comparison between modeling and experimental heat release rate for Diesel

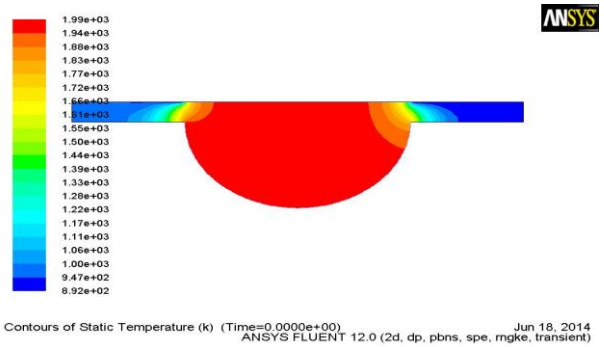

Figure 10. Temperature distribution in (K) CA = 360^0 (maximum load) for biodiesel blend

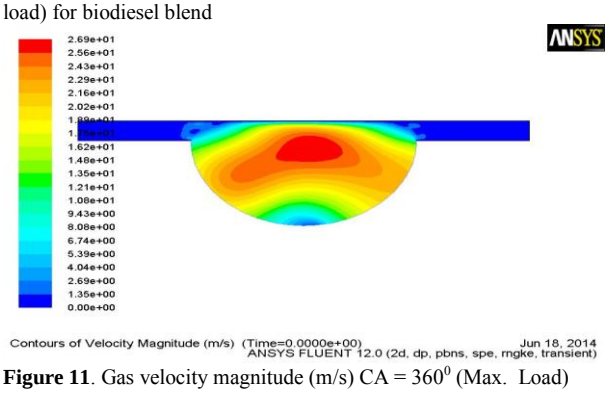

Figure 11. Gas velocity magnitude (m/s) CA = 360^0 (Max. Load) for biodiesel blend.

7. Results and Discussion

Figures 4 and 5 show modeling and experimental max. in-cylinder pressure traces operating at full load condition. The modelled cylinder pressure data show a good agreement with the experimental results. The maximum pressure rise depends upon the quantity of fuel vaporized during the delay time and occurs in the state of combustion, some degrees after the beginning of the combustion. Note that the modeling peak pressure was 47 bar at 360 degree CA, and the experimental peak pressure was 45 bar at 360 degree CA for biodiesel. Therefore, both scale and timing of occurrence of peak pressure were precisely predicted by the model. The observed cylinder pressure profiles reflect the effect of the in-cylinder heat release rate. The heat release rate was determined from pressure data. Figures 8 and 9 compare the heat release rates computed from modeling and experimental pressure traces. The heat release rate decreases from the start of injection to the start of combustion which was the ignition delay period because of the fuel evaporation occurring during this period. The first peak, due to premixed combustion, strongly depends on the amount of the fuel prepared for combustion during the ignition delay period. The second peak, due to diffusion combustion, was controlled by the fuel air mixing rate. Diffusion combustion continues until the combustion is completed. Note that the peak modeling heat release rate was 30 J/s whereas the experimental peak heat release rate was 25 J/s at 364 degree CA for biodiesel. Figure 4 shows the comparison of the measured and CFD modelled cylinder pressures.

The peak pressure and the pressure gradient over the combustion period produced by CFD simulation match closely with experimental. The peak cylinder pressure was over predicated by about 4%. Also, from heat release rate graph, the experimental validation of combustion is shown. Figure 7 shows the temperature contour diagram at maximum loads. This shows that increasing the load, which corresponds to increasing the fuel mass flow rate, results in increasing the combustion temperature. The Figure shows that the temperature of the air at the end of compression was sufficiently high for the droplets of fuel to vaporize and ignite as they enter the cylinder. The maximum temperature that occurs in case of biodiesel was 1990 K. Figure 8 shows the velocity magnitude contour for biodiesel and diesel fuel respectively. The velocity magnitude of diesel was 18 m/s while biodiesel had 26 m/s. This difference was due to the variation in viscosity according to the change in temperature and pressure of diesel and biodiesel as given in Table 2. Also, there were changes in the velocity contour of diesel and biodiesel because of their chemical characteristics.

8. Conclusion

The CFD code FLUENT was used to simulate the combustion characteristics of direct injection diesel engine fuelled with biodiesel blend. The fluid flow in DI diesel has bowel in piston with turbulence and combustion processes modelled with sufficient generality to include spray formation, delay period, chemical kinetics and onset of ignition. A good agreement between the modeling and experimental data ensures the accuracy of the numerical predictions collected in this work. The model was validated through the comparison of the predicted p-θ curve with the experimental p-θ curves and heat release rate. It shows that CFD can be a reliable tool for the

combustion modelling of CI engine fuelled with biodiesel blend. Pongamia Pinnata biodiesel blend can be a suitable replacement to diesel; hence it can be used as an alternative fuel for a future work.

References

[1] B. Jayashankara, V.Ganesan, "Effect of fuel injection timing and intake pressure on the performance of a DI diesel engine – A parametric study using CFD". Elsevier, Energy Conversion and Management 51 (2010), 1835–1848.

[2] Devershi Mourya,Vivek Roy, "Combustion modelling and simulation of combustion emissions for diesel engine operating on the blends of jatropha biodiesel and diesel", IJEST, Vol. 4 (2012), No. 4, 1373-1381.

[3] D. Deshmukh, R.V. Ravikrishna, "experimental studies on high-pressure spray structure of biofuels". Atomization and Sprays Vol. 21 (2011), No. 6, 467–481.

[4] F. Payri, J. Benajes, "CFD modeling of the in-cylinder flow in direct-injection Diesel engines". Elsevier, Computers & Fluids 33 (2004), 995–1021.

[5] Hoon Kiat Ng, Suyin Gan, "Simulation of biodiesel combustion in a light-duty diesel engine using integrated compact biodiesel–diesel reaction mechanism". Elsevier, Applied Energy, Vol. 102 (2013), 1275–1287.

[6] L. Saravanakumar, Ramesh Bapu B.R., "Analysis and Effect of Squish Generation Using CFD on Variable Compression Ratio C.I Engine". IJERT, Vol. 2 (2013), Issue 9, 1757-1764.

[7] Ming Jia, Maozhao Xie, "The effect of injection timing and intake valve close timing on performance and emissions of diesel PCCI engine with a full engine cycle CFD simulation". Elsevier, Applied Energy 88 (2011), 2967–2975.

[8] P. Jonathon, McCrady, Valerie L. Stringer, "Computational analysis of biodiesel combustion in a low-temperature combustion engine using well-defined fuel properties". 07 PFL - 655 (2007) SAE International.

[9] R.Adnan, H.H. Masjuki, "Computational simulation and prediction on the performance and emissions of dual fuel diesel engine operated with pilot diesel fuel and hydrogen gas". International conference, ICCBT 2008, 95-102.

[10] R. Mikalsen, A.P. Roskilly, "A computational study of free-piston diesel engine combustion". Sir Joseph Swan Institute for Energy Research, Newcastle University, New castle upon Tyne, NE1 7RU, United Kingdom.

[11] Renganathan Manimaran, Rajagopal Raj, K. Senthil Kumar, "Numerical Analysis of Direct Injection Diesel Engine Combustion using Extended Coherent Flame 3-Zone Model". Research Journal of Recent Sciences, Vol. 1 (2012), No.8, 1-9.

[12] Shaik Magbul Hussain, "CFD analysis of combustion and emissions to study the effect of compression ratio and biogas substitution in a diesel engine with experimental verification". IJEST, Vol. 4, (2012), No. 2, 473-492.

[13] S. Som, D.E. Longman, "Numerical study comparing the combustion and emission characteristics of biodiesel to petro-diesel". American chemical society, ACS publications, Energy Fuels, 25 (2011), 1373–1386.

[14] T. Reinhard, P. Peter, "3D-CFD simulation of DI diesel engine combustion and pollutant formation". Scientific Bulletin Faculty of Mechanics and Technology Automotive series, year XVI, No.20.

[15] S.M. Jameel Basha, "simulation of in-cylinder processes in a di diesel engine with various injection timings, ARPN journal of engineering and applied sciences". Vol. 4 (2009), No. 1, 1-7.

[16] T.M. Belal, Sayed M. Marzouk, "Investigating Diesel Engine Performance and Emissions Using CFD". Scientific research, Energy and Power Engineering, 5 (2013), 171-180.

[17] U.V. Kongre, V.K.Sunnapawar, "CFD modelling and experimental validation of combustion in direct injection engine fueled with diesel". IJAER, Dindigul, Vol. 1 (2010), No. 3, 508-517.

[18] Heywood J. B. Internal combustion engine fundamentals, McGraw-Hill, 1988, p. 102-230.

[19] Stephen R T, An introduction to combustion: concepts and applications, McGraw-Hill, 1996, p. 56-191.